CANCER GENOMICS & PROTEOMICS 6: 161-176 (2009)

# Gene Expression Analysis of HCT116 Colon Tumor-derived Cells Treated with the Polyamine Analog PG-11047

NATALIA A. IGNATENKO[1], HAGIT F.YERUSHALMI[2], RITU PANDEY[3], KAREN L.KACHEL[4], DAVID E. STRINGER[4], LAURENCE J. MARTON[5] and EUGENE W. GERNER[1,6]

*Departments of [1]Cell Biology and Anatomy, [3]Bioinformatics Core, Arizona Cancer Center, [4]Cancer Biology Division, and [6]Biochemistry and Molecular Biophysics, Arizona Cancer Center, The University of Arizona, Tucson, AZ, U.S.A.; [2]Skin Research Laboratory, The Ruth and Bruce Rappaport Faculty of Medicine, Technion - Haifa, Israel; [5]Progen Pharmaceuticals, Inc., Redwood City, CA, U.S.A.*

**Abstract.** *Background: The conformationally restricted polyamine analog PG-11047 has significant growth inhibitory activity against prostate and lung cancer cell lines and is currently under evaluation in several clinical trials, both alone and in combination with other drugs, for the treatment of relapsed or refractory cancer. The objective of this study was to identify the molecular signature of genes responsive to PG-11047 treatment and the biochemical effects of this drug in the HCT116 colon cancer cell line. Materials and Methods: Gene expression analysis was performed using Affymetrix GeneChip human genome U133 Plus 2.0 arrays. Changes in protein expression were evaluated using 2D polyacrylamide gels followed by LCMS/MS. Results: Treatment of cells with PG-11047 at concentrations ranging from 0.1 to 10 μM caused inhibition of cell growth. The activity of PG-11047 was found to correlate with its transcriptional effects on cell cycle control, focal adhesion, adherent and gap junction genes, MAPK-, Wnt- and, TGF-β signaling pathways, transport and DNA/RNA transcription factor genes. PG-11047 caused depletion of polyamine pools. Proteomics analysis showed that PG-11047 restricts the modification of eukaryotic translation initiation factor 5A (eIF5A), resulting in suppression of general protein synthesis in PG-11047-treated cells. Conclusion: These data show that PG-11047 has a broad spectrum of anticancer activity in colon cancer cells.*

*Abbreviations:* ODC, Ornithine decarboxylase; EGR-1, early growth response gene-1; SAT1, spermine/spermidine $N^1$-acetyltransferase; eIF5A, eukaryotic translation initiation factor 5A.

*Correspondence to:* Natalia A. Ignatenko, Ph.D., The University of Arizona, Arizona Cancer Center, 1515 N. Campbell Avenue, Tucson, AZ 85724, U.S.A. Tel: +1 5206268044, Fax: +1 5206264480, e-mail: nignatenko@azcc.arizona.edu

*Key Words:* Polyamine analogs, PG-11047, colon cancer cells, Affymetrix gene chip microarray, polyamines.

Polyamines are small polycations that are necessary for cell proliferation (1-3). Polyamines have been shown to influence transcription (4), RNA stabilization and translational frameshifting (5). The cellular functions of polyamines include intestinal mucosal maturation (6) and cell migration (7). Intracellular polyamine concentrations and activity of a key polyamine biosynthetic enzyme, ornithine decarboxylase (ODC), are elevated in colorectal cancer tissues and in premalignant polyps of cancer patients (8). Polyamine metabolism is up-regulated in intestinal epithelial tissues in humans with familial adenomatous polyposis (FAP), a syndrome caused by mutations in the adenomatous polyposis coli (*APC*) tumor suppressor gene and associated with a high risk of colon and other types of cancer (9). APC signaling regulates ODC expression in both human cells and a mouse model of FAP (10, 11). The irreversible inhibitor of the ODC gene, α-difluoromethylornithine (DFMO) suppresses intestinal polyamine levels and tumor formation in experimental models of colon cancinogenesis (10, 12, 13). DFMO has been evaluated in several clinical trials for the prevention of skin and colon cancer precursors and in men with familial risk of prostate cancer (14-17). In spite of the positive results, the activity of DFMO *in vivo* is limited because of the compensatory increase in cellular transport of polyamines available from the diet and gastrointestinal flora. The use of structural polyamine analogs represents a complementary approach to inhibition of polyamine biosynthesis in cells (18). Mechanisms by which polyamine analogs exert their intracellular effects include the induction of polyamine catabolic enzyme spermidine/spermine $N^1$-acetyltransferase, depletion of intracellular polyamine pools, competition with natural polyamines for uptake, and the displacement of natural polyamines from functional sites related to the transcriptional regulation of genes (19, 20). Three classes of synthetic polyamine analogs have been developed and include symmetrically substituted, asymmetrically substituted and conformationally restricted

analogs. These classes demonstrate multiple biological activities and improved targeting abilities with small changes in molecular structure (19). We previously investigated the molecular mechanisms of the antineoplastic activity of a member of the second generation of polyamine analogs, PG-11093 (formerly CGC-11093) (21). We showed that the activity of PG-11093 is attributed to its transcriptional regulation of cell cycle control, transforming growth factor, (TGF)-β signaling, transport and DNA/RNA transcription factor genes.

PG-11047 is another second-generation conformationally restricted polyamine analog, whose structure is based on the symmetrically alkylated analog N1, N11-*bis* (ethyl) norspermine (BENSpm) but which is modified by the introduction of a double bond into the central 4-carbon methylene chain (22, 23). Antiproliferative activity of PG-11047 has been reported against human breast cancer cells and both small cell and non-small cell lung cancer cell lines (24-26). PG-11047 significantly delayed the development of A549 xenografts in nude *nu/nu* mice (24). The biochemical mechanisms of the antitumor effects of PG-11047 include the cell type-specific down-regulation of ODC and the induction of SAT1 activities, and the antizyme-mediated feed-back inhibition of polyamine uptake (24, 27). PG-11047 is currently being tested in a Phase I clinical trial in patients with relapsed or refractory cancer as a single agent and in a Phase Ib trial in combination with bevacizumab (Avastin®; Genentech (South San Francisco, CA, USA)), erlotinib (Tarceva®; OSI Pharmaceuticals Inc., Long Island, NY, USA), docetaxel (Taxotere®; Sanofi-Aventis, Paris, France), gemcitabine (Gemzar®; Eli Lilly, Indianapolis, IN, USA), 5-fluorouracil (5-FU), cisplatin, or Sutent (http://www.cancer.gov/search/ResultsClinicalTrialsAdvanced.aspx?protocolsearchid=335980.

It has been shown that periocular injections of PG-11047 in mice causes significant suppression and regression of laser-induced choroidal neovascularization (CNV), of oxygen-induced ischemic retinopathy, or of neovacularization in transgenic mice overexpressing vascular endothelial growth factor (VEGF) in photoreceptors, indicating its antiangiogenic properties and the possibility of its use clinically (28).

In this study, we evaluated the molecular and biochemical effects of PG-11047 in the colon adenocarcinoma cell line HCT116 on the expression of growth-promoting genes and signaling pathways affected by this drug. We also report the effect of this drug on general protein synthesis in HCT116 cells.

## Materials and Methods

*Chemicals and reagents*. All culture reagents were obtained from Invitrogen Corp. (Carlsbad, CA, USA). An RNeasy kit was purchased from Qiagen Inc. (Valencia, CA, USA) and a Reverse Transcription Kit was purchased from Promega Corp. (Madison, WI, USA). Invitrogen Corp. synthesized all oligonucleotides used in the experiments. All reagents for real time RT-PCR were purchased from Applied Biosystems, Inc. (Foster City, CA, USA). [1,8,-$^{3}$H]Spermidine and [$^{35}$S]-methionine were purchased from PerkinElmer Life Science (Boston, MA, USA). N1-Guanyl-1,7-diaminoheptane (GC-7) was purchased from Biosearch Technologies, Inc. (Novato, CA, USA). DFMO was generously donated by Ilex Oncology Inc. (San Antonio, TX, USA).

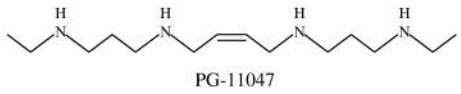

PG-11047

Figure 1. *Structure of PG-11047.*

*PG-11047*. The polyamine analog PG-11047 was obtained from Progen Pharmaceuticals, Inc. (Redwood City, CA, USA). PG-11047 ([$^{1}$*N*,$^{12}$*N*]*bis*(ethyl)-*cis*-6,7-dehydrospermine tetrahydrochloride) is a bisethyl spermine analog conformationally restricted due to the presence of a double bond (Figure 1). PG-11047 was synthesized as described elsewhere (22, 23). PG-11047 is highly water-soluble and a stock solution (10 mM) was prepared in water, sterile-filtered, and stored at –20˚C. Further dilutions were made in complete growth medium.

*Cell culture*. HCT116 colon adenocarcinoma cell line was purchased from American Type Culture Collection (ATCC) (Rockville, MD, USA) and was maintained in Dulbecco's modified Eagle's medium (DMEM) supplemented with 10% fetal bovine serum (FBS) and 1% penicillin/streptomycin.

*Cell viability*. Cells were seeded at a density of $0.25\times10^{6}$ cells per 60 mm dish in media containing different concentrations of PG-11047 (0.1, 1, 10 or 50 μM) and were collected at various times after subculture, as indicated in the figures. The viability of control and analog-treated cells was evaluated by an automated Trypan blue dye exclusion method using a Beckman Coulter Vi-Cell™ Cell Viability analyzer (Beckman Coulter Inc, Miami, FL, USA).

*Isolation of total RNA and reverse transcription*. HCT116 cells were seeded in the absence or presence of PG-11047 at either 1 μM or 10 μM for 72 h. Total cellular RNA was extracted according to a protocol supplied with the Qiagen RNeasy Kit. RNA samples were evaluated for integrity of 18S and 28S rRNA by ethidium bromide staining of 1 μg of RNA resolved by electrophoresis in a 1.0% agarose/formaldehyde gel. Reverse transcription was completed using a TaqMan Reverse Transcription Reagents Kit. Two μg of total RNA were transcribed into cDNA in a 100 μl reaction using Random hexamers and the recommended thermal conditions. The RNA from control and PG-11047-treated HCT116 cells was isolated from three independent experiments with different cell passages (taken from passages 54-60).

*Microarray analysis*. Ten μg of total RNA were used to produce biotinylated cRNA that was hybridized to the Affymetrix GeneChip® human genome U133 Plus 2.0 array according to the manufacturer's instructions (Affymetrix Inc., Santa Clara, CA, USA). Chips were washed and stained using a Fluidics Station (Affymetrix) and scanned with a GeneArray Scanner 3000 using

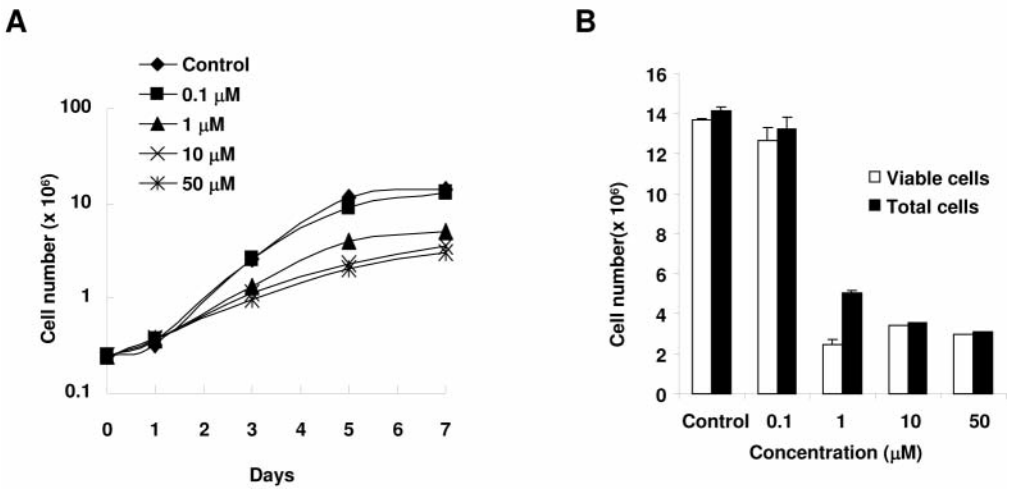


Figure 2. *Effect of PG-11047 treatment on the growth and viability of HCT116 colon cancer cells. A, Compound was added to cells to a final concentration of 0.1, 1, 10, or 50 μM. Cells were collected on different days after subculture and total cell numbers were determined. Results shown represent the means of duplicate determinations in a single representative experiment that was replicated once. B, HCT116 cell viability on day 7 after subculture. Control cells and cells seeded in medium containing different concentrations of PG-11047 were cultured for seven days. Cells were harvested, and the percentage of viable cells was determined using an automated trypan blue dye exclusion method. Data presented are the average of three independent experiments.*

default settings. Images from the scanned chips were quantifed to produce transcript level data using the Affymetrix Microarray Analysis Suite (MAS) 5.0. Transcript level data were loaded into GeneSpring 7.0 (Agilent Technologies, Santa Clara, CA, USA) and normalized across arrays. Fold change was derived as the ratio of average differences from three experimental arrays as compared to three control arrays. Genes were selected based on analysis of variance (ANOVA) with variances not assumed equal (Welch's ANOVA) and a *p*-value of 0.05 adjusted for multiple testing using the Benjamini Hochberg false discovery rate method. A global error model based on replicates of the control and treated samples was used to estimate variance.

*Quantitative real-time RT-PCR*. Real-time PCR amplification was performed with an ABI PRISM 7700 SDS instrument (Applied Biosystems), utilizing the universal thermal cycling conditions recommended by the Assay-on-Demand products protocol. Each 50 μl reaction included 25 μl of TaqMan Universal PCR master mix, 5 μl of the resulting cDNA from the reverse transcription step, and 20 μl diluted primer and probe mixes ordered from Assay-on-Demand products (Applied Biosystems). No template controls were included in each plate to monitor potential PCR contamination. The drug effect on target genes was tested in triplicate and each reaction was run in duplicate. To determine the relative expression level of each target gene, the comparative $C_T$ method was used. The $C_T$ value of the target gene was normalized by the endogenous reference ($\Delta C_T = C_{T(target)} - C_{T(GAPDH)}$) and compared with a calibrator ($\Delta\Delta C_T = \Delta C_{T(target)} - \Delta C_{T(calibrator)}$). The first of three HCT116 replicates was designated as the calibrator sample in these experiments. The relative expression of each target gene was calculated *via* the equation $2^{-\Delta\Delta CT}$. Data were presented as a ratio of the relative expression of each target gene in drug-treated cells to the expression of this gene in the first control replicate.

*Pathway analysis and visualization*. The set of genes with 3-fold changes in expression in response to 10 μM PG-11047 was searched against Pathway Miner (29) to identify cellular pathways influenced by PG-11047 treatment. Pathway Miner is a web-based interactive tool, written in Perl and Java, that provides expression patterns for affected pathways from 3 different pathway resources: KEGG (www.genome.ad.jp), BioCarta (www.biocarta.com) and GenMAPP (www.genmapp.org). The tool provides multiple outputs for interpretation of pathway perturbations. The expression patterns represented on pathways are based on a fold-change color scheme. The gene association network displays genes that collectively influence or participate in one or more pathways. In the network, nodes represent genes and the edges represent pathways. The thickness of the edge represents number of pathways to which the two connecting genes belong.

*ODC enzyme activity*. ODC activity was determined by measuring the liberation of $^{14}CO_2$ from L-[$^{14}$C]ornithine (DuPont-New England Nuclear (Wilmington, DE, USA)), as described by Sertich *et al*. (30).

*Polyamine measurement*. Cells were grown with PG-11047 (10 μM) for 24 and 48 hours. Cell extracts were prepared in 0.1 N HCl in a proportion of $1\times10^7$ cells per 900 μl. Samples were sonicated, adjusted to 0.2 N $HClO_4$ and incubated on ice for 2 h. After centrifugation at 13,000× *g* for 10 min at 4˚C, the supernatants were analyzed by reverse-phase high-performance liquid chromatography with 1,7-diaminoheptane as an internal standard (31).

*Proteomics analysis*. Seventy-two hours after subculture, control and PG-11047 treated cells (10 μM) were lysed on ice in radioimmunoprecipitation assay (RIPA) buffer (PBS, 1% NP-40, 0.5% sodium deoxycholate, 0.1% SDS, 30 μg/ml aprotinin, 100 mM sodium orthovanadate, and a 10 mg/ml phenylmethylsulfonyl fluoride), sonicated for 5-10 s and then incubated on ice for 30 min.

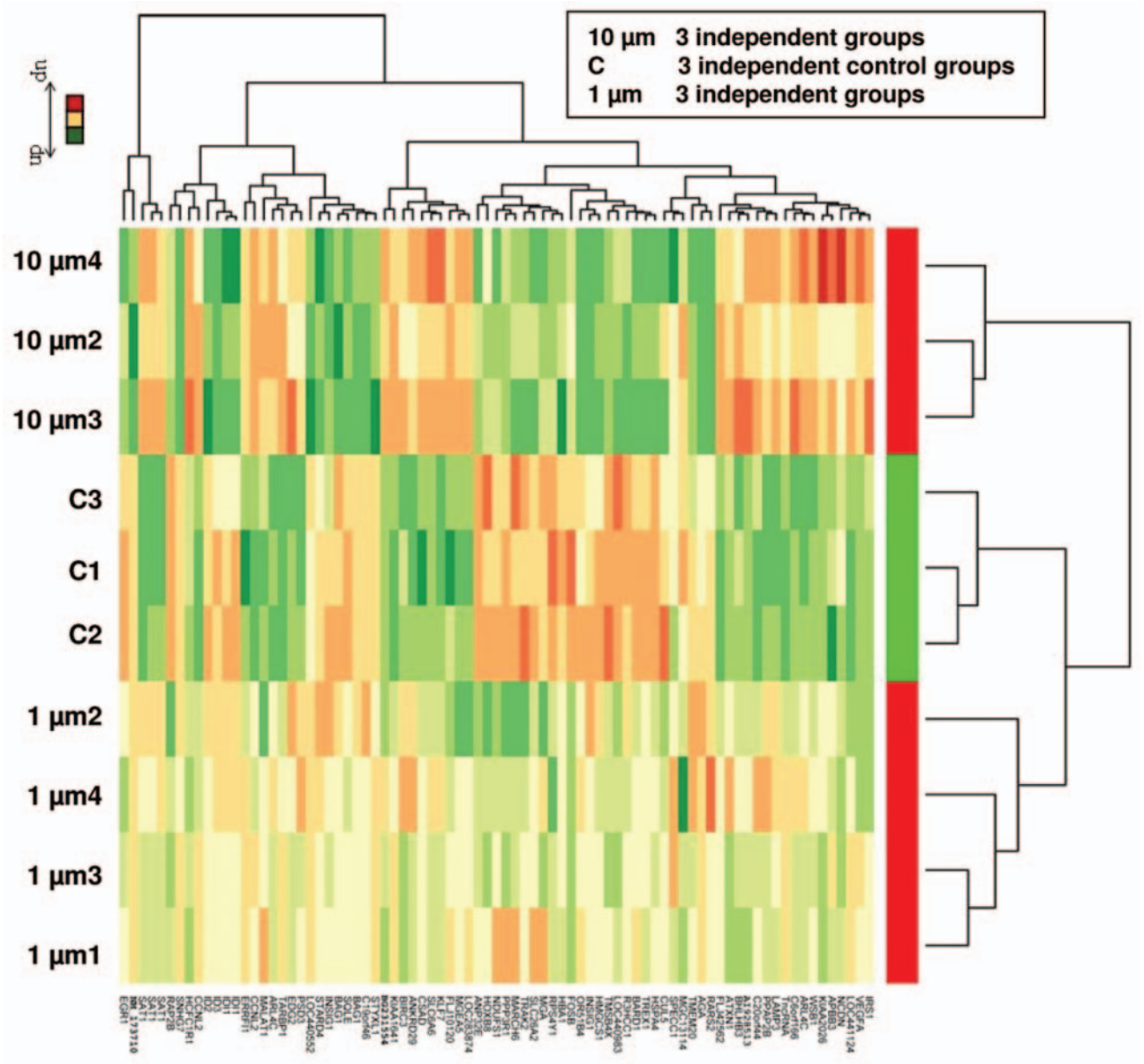


Figure 3. *Heatmap of 81 genes found to be significantly changing with 10 µm treatment. Bioconductor was used to generate the heatmap. The row names show the gene names and where gene names are not available accession numbers are given. Gene expressions are shown as varying level of colors red and green, with red for up-regulation and green for down-regulation.*

Lysates were centrifuged at 13,000 rpm 4˚C for 20 min. Supernatants were collected and cleaned using a ReadyPrep 2D Cleanup Kit (Bio-Rad Laboratories, Hercules, CA, USA). Protein concentration was determined using a Bio-Rad $D_C$ protein assay (BioRad). Samples were analyzed by the Proteomics Facility Core (University of Arizona) using 2D PAGE gel electrophoresis (pI 5-8, 10-20% gradient). The gels were silver stained, followed by in-gel digestion of spots expressed exclusively in one of the samples (control or PG-11047-treated). The samples were analyzed using nanoLC-MS/MS and SEQUEST database searching.

*VEGF Western blotting*. Seventy-two hours after subculture, control and PG-11047-treated cells (1 µM and 10 µM) were lysed with a RIPA buffer. Samples were kept on ice for 30 min, followed by centrifugation at 13,000× *g* for 10 min. Supernatants were collected and protein concentration was determined with the Bio-Rad DC protein assay. A total of 80 µg of cell lysate was loaded per lane and run on a 15% SDS-PAGE gel. The proteins were transferred electrophoretically to Hybon-C nitrocellulose membrane (Amersham Pharmacia Biotech, Inc., Piscataway, NJ, USA) overnight. Blots were blocked in Blotto A (5% w/v nonfat dry-milk,

Table IA. *List of genes statistically significantly altered by ≥3-fold in response to PG-11047 (10 μm).*

| Gene ID | Symbol | Description | Fold change Mean±SD |
|---|---|---|---|
| Systematic | ANP32E | Acidic (leucine-rich) nuclear phosphoprotein 32 family, member E | 0.108±0.042 |
| 229128_s_at | PRPS2 | Phosphoribosyl pyrophosphate synthetase 2 | 0.175±0.034 |
| 230352_at | | --- | 0.183±0.044 |
| 238199_x_at | EGR1 | Early growth response 1 | 0.189±0.070 |
| 227404_s_at | ID3 | Inhibitor of DNA binding 3, dominant negative helix-loop-helix protein | 0.177±0.031 |
| 207826_s_at | | Homeo box B8 | 0.220±0.128 |
| 229667_s_at | MTND3 | --- | 0.224±0.087 |
| 1553588_at | INSIG1 | Insulin-induced gene 1 | 0.198±0.011 |
| 201625_s_at | BAG1 | BCL2-associated athanogene | 0.221±0.058 |
| 211475_s_at | SQLE | Squalene epoxidase | 0.211±0.042 |
| 213577_at | LOC203069 | Hypothetical protein LOC203069 | 0.233±0.078 |
| 212866_at | INSIG1 | Insulin-induced gene 1 | 0.196±0.042 |
| 201627_s_at | ID2 | Inhibitor of DNA-binding 2, dominant negative helix-loop-helix protein | 0.235±0.057 |
| 201565_s_at | FOSB | FBJ murine osteosarcoma viral oncogene homolog B | 0.181±0.024 |
| 202768_at | | --- | 0.275±0.063 |
| 234469_at | STARD4 | START domain containing 4, sterol-regulated | 0.217±0.071 |
| 226390_at | NDUFS1 | NADH dehydrogenase (ubiquinone) Fe-S protein 1, 75 kDa (NADH-coenzyme Q reductase) | 0.263±0.075 |
| 236356_at | RPS4Y | Ribosomal protein S4, Y-linked | 0.248±0.031 |
| 201909_at | TREX1 | Three prime repair exonuclease 1 | 0.257±0.024 |
| 205875_s_at | IDI1 | Isopentenyl-diphosphate delta isomerase | 0.228±0.041 |
| 204615_x_at | THRAP3 | Thyroid hormone receptor-associated protein, 150 kDa subunit | 0.285±0.127 |
| 227338_at | | *Homo sapiens* mRNA; cDNA DKFZp564P142 (from clone DKFZp564P142) | 0.229±0.040 |
| 221750_at | TEB4 | Similar to *S. cerevisiae* SSM4 | 0.280±0.062 |
| 201737_s_at | HSPA4 | Heat-shock 70 kDa protein 4 | 0.274±0.037 |
| 208814_at | HBA2 | Hemoglobin, alpha 2 hemoglobin, alpha 2 | 0.290±0.087 |
| 211699_x_at | RARSL | Arginyl-tRNA synthetase-like | 0.310±0.075 |
| 1561048_at | AGA | Aspartylglucosaminidase | 0.309±0.042 |
| 216064_s_at | IDI1 | Isopentenyl-diphosphate delta isomerase | 0.252±0.035 |
| 208881_x_at | CUL5 | Cullin 5 | 0.317±0.092 |
| 230393_at | | Amyotrophic lateral sclerosis 2 (juvenile) chromosome region, candidate 3 | 0.327±0.095 |
| 202124_s_at | BAG1 | BCL2-associated athanogene | 0.329±0.002 |
| 202387_at | | Protein phosphatase 3 (formerly 2B), regulatory subunit B, 19 kDa, alpha isoform (calcineurin B, type I) | 0.324±0.069 |
| 204506_at | TMEM20 | Hypothetical protein FLJ33990 | 0.313±0.044 |
| 236219_at | | *Homo sapiens* cDNA FLJ37115 fis, clone BRACE2022158. | 0.307±0.022 |
| 1562849_at | MGA | MAX gene associated | 0.307±0.079 |
| 235409_at | FLJ36445 | Hypothetical protein FLJ36445 | 0.328±0.053 |
| 235515_at | MGC13114 | Hypothetical protein MGC13114 | 0.321±0.002 |
| 227380_x_at | SLC26A2 | Solute carrier family 26 (sulfate transporter), member 2 | 0.320±0.088 |
| 205097_at | RAP2B | RAP2B, member of RAS oncogene family | 0.318±0.069 |
| 227897_at | MGC16037 | Hypothetical protein MGC16037 | 0.326±0.046 |
| 229050_s_at | MK-STYX | Map kinase phosphatase-like protein MK-STYX | 0.330±0.073 |
| 233982_x_at | BARD1 | BRCA1-associated RING domain 1 | 0.339±0.096 |
| 205345_at | EFA6R | ADP-ribosylation factor guanine nucleotide factor 6 | 2.875±0.412 |
| 203355_s_at | BHLHB3 | Basic helix-loop-helix domain containing, class B, 3 | 3.108±0.807 |
| 221530_s_at | HCFC1R1 | Host cell factor C1 regulator 1 (XPO1 dependant) | 3.002±0.461 |
| 45714_at | LAMP3 | Lysosomal-associated membrane protein 3 | 3.268±0.476 |
| 205569_at | KIAA1641 | KIAA1641 protein | 3.270±0.404 |
| 214723_x_at | KIAA2026 | KIAA2026 | 3.008±0.659 |
| 238490_at | IRS1 | Insulin receptor substrate 1 | 3.051±0.478 |
| 235392_at | SLC6A6 | Solute carrier family 6 (neurotransmitter transporter, taurine), member 6 | 3.042±0.766 |
| 205921_s_at | EDG2 | Endothelial differentiation, lysophosphatidic acid G-protein-coupled receptor, 2 | 3.011±0.888 |
| 204036_at | | *Homo sapiens* similar to hypothetical protein DKFZp434F142 (LOC339494), mRNA | 3.053±0.692 |
| 227922_x_at | BIRC3; AIP1; API2; MIHC; CIAP2; HAIP1; HIAP1; RNF49 | Baculoviral IAP repeat-containing 3 baculoviral IAP repeat-containing 3 | 3.044±0.845 |

Table I. *continued*

Table IA. *continued*

| Gene ID | Symbol | Description | Fold change Mean±SD |
|---|---|---|---|
| 210538_s_at | TARBP1 | TAR (HIV) RNA binding protein 1 | 3.228±0.555 |
| 202813_at | APBB3 | Amyloid beta (A4) precursor protein-binding, family B, member 3 | 3.148±0.287 |
| 204650_s_at | SCA1 | Spinocerebellar ataxia 1 (olivopontocerebellar ataxia 1, autosomal dominant, ataxin 1) | 3.272±0.550 |
| 203232_s_at | KLF7 | Kruppel-like factor 7 (ubiquitous) | 3.068±0.872 |
| 1555420_a_at | | *Homo sapiens* transcribed sequences | 3.389±0.524 |
| 229672_at | PPAP2B | Phosphatidic acid phosphatase type 2B | 3.325±0.563 |
| 212230_at | FLJ10120 | Hypothetical protein FLJ10120 | 3.074±0.217 |
| 220220_at | CCNL2 | Cyclin L2 | 3.589±0.570 |
| 222999_s_at | | Chromosome 6 open reading frame 166 | 3.315±0.663 |
| 227368_at | VEGF | Vascular endothelial growth factor | 3.519±0.805 |
| 211527_x_at | ARL7 | ADP-ribosylation factor-like 7 | 3.112±0.689 |
| 202206_at | CSAD | Cysteine sulfinic acid decarboxylase | 3.259±0.549 |
| 221139_s_at | NCDN | Neurochondrin | 3.8422±3.795 |
| 209556_at | | *Homo sapiens* transcribed sequences | 3.831±0.481 |
| 227985_at | ARL7 | ADP-ribosylation factor-like 7 | 3.945±0.715 |
| 202207_at | | *Homo sapiens* mRNA; cDNA DKFZp686J1595 (from clone DKFZp686J1595) | 3.695±0.639 |
| 243179_at | | *Homo sapiens* mRNA; cDNA DKFZp686L01105 (from clone DKFZp686L01105) | 3.296±0.649 |
| 238320_at | CCNL2 | Cyclin L2 cyclin L2 | 4.441±0.130 |
| 221427_s_at | SAT | Spermidine/spermine $N^1$-acetyltransferase | 3.809±1.010 |
| 203455_s_at | LOC283874 | *Homo sapiens*, clone IMAGE:5296395, mRNA | 4.057±0.631 |
| 1563629_a_at | MGEA5 | Meningioma expressed antigen 5 (hyaluronidase) | 4.899±0.778 |
| 235868_at | LOC147463 | Hypothetical protein LOC147463 | 4.883±1.748 |
| 238332_at | SAT | Spermidine/spermine $N^1$-acetyltransferase | 5.220±1.188 |
| 210592_s_at | WSB1 | SOCS box-containing WD protein SWiP-1 | 5.433±1.205 |
| 201294_s_at | PRO1073 | PRO1073 protein | 6.610±1.276 |
| 224558_s_at | SAT | Spermidine/spermine $N^1$-acetyltransferase | 6.462±1.897 |
| 213988_s_at | | *Homo sapiens* transcribed sequences | 5.819±1.239 |
| 235419_at | | *Homo sapiens* similar to hypothetical protein MGC38936 (LOC344403), mRNA | 6.537±2.286 |

Table IB. *Top 5 known genes altered after treatment with 10 μM of PG-11047 with at least 3-fold change ($p<0.05$) and validated using real time RT PCR.*

| Gene name, symbol, and accession number | Fold change at 1 μM Mean±SD | Fold change at 10 μM Mean±SD | Function |
|---|---|---|---|
| Early growth response 1, EGR1, AI459194 | 0.33±0.14 | 0.19±0.07 | Transcriptional regulator, recognizes and binds to the DNA sequence 5'-CGC CCC CGC-3' (EGR response element). Activates the transcription of target genes whose products are required for mitogenesis and differentiation |
| Cyclin L2, CCNL2, NM_03093 | 2.51±0.53 | 3.59±0.57 | Regulates transcription and RNA processing of apoptosis-related fuctors, resulting in tumor growth inhibition and apoptosis |
| Spermidine/spermine N1 acetyltransferase, SAT, M55580 | 3.36±1.89 | 6.46±1.9 | Key polyamine catabolic enzyme, catalyzes the acetylation of polyamines. It is also involved in the regulation of polyamine transport out of cells |
| Solute carrier family 6, member A6, SLC6A6, U16120 | 1.46±0.37 | 3.04±0.77 | Neurotransmitter, taurine transporter |
| Vascular endothelial growth factor, VEGF-A, M27281 | 2.21±0.5 | 3.52±0.8 | Growth factor active in angiogenesis, vasculogenesis and endothelial cell growth. Promotes cell migration, inhibits apoptosis |

0.1% Tween 20, and Tris-buffered saline (TBS) consisting of 10 mM Tris-HCl, pH 8.0, 150 mM NaCl) for 1 hour at room temperature. A mouse anti-VEGF monoclonal antibody (C-1) (Cat.# sc-7269; Santa Cruz, CA, USA) was used at a dilution of 1:100 and incubated overnight at 4˚C. The blots were washed in TBS/0.1% Tween-20. The primary antibodies were detected with an anti-mouse immunoglobulin G antibody conjugated to horseradish peroxidase for 1 h at room temperature. Blots were washed as described above and protein was detected with enhanced chemiluminescence detection reagent (Amersham). Western blotting was repeated three times and quantified using Scion Imaging Quantification Software (Scion Corp., Frederick, MD, USA).

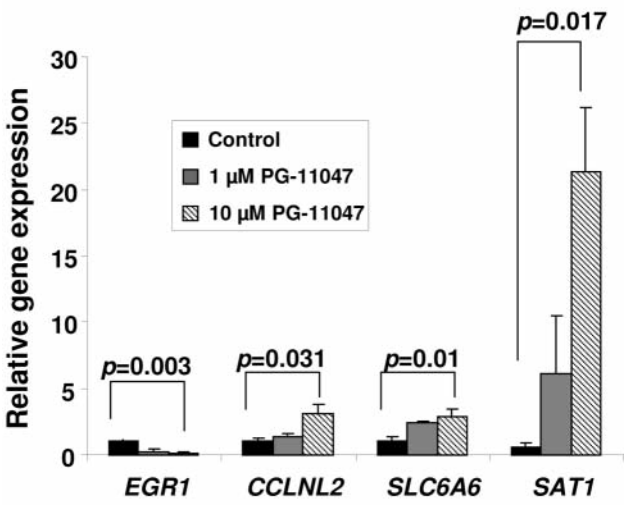


Figure 4. *Validation of PG-11047-dependent changes in gene expression by real-time RT-PCR. HCT116 cells were grown without (control) or in the presence of 10 μM PG-11047 for 72 h. Cells were harvested and total RNA was extracted according to a protocol supplied with the Qiagen RNeasy kit. RT and real-time PCR were performed as described in Materials and Methods. Individual bars represent the relative expression of each validated gene in treated cells to the expression of this gene in the control cells. Results are presented as average values of three independent experiments. P-values between control and treated cells were calculated with t-test.*

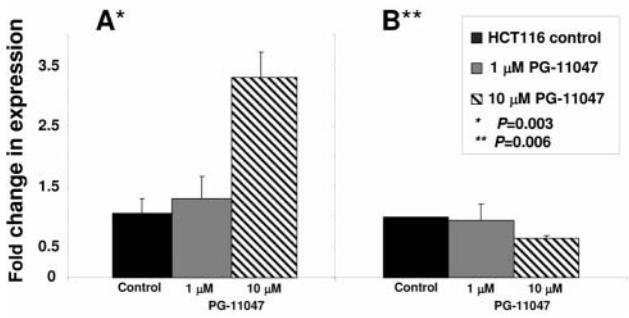


Figure 5. *VEGF transcript and protein levels in PG-11047-treated HCT116 cells. Cells were grown without (control) or in the presence of 10 μM PG-11047 for 72 h and collected for real-time PCR analysis (A) and Western blot analysis (B) as described in Materials and Methods. Results are presented as average values of three independent experiments. P-values between control and treated cells were calculated with t-test.*

*Analysis of hypusine production using HPLC*. Hypusine was quantified using a high performance liquid chromatography method described elsewhere (32). Briefly, after growing cells in 100 mm dishes for 24 hours, they were treated with 5 mM DFMO for 48 hours to suppress endogenous spermidine and cause unmodified eIF5A to accumulate. Aminoguanidine 1 mM, which inhibits serum amine oxidases, and 10 μM PG-11047 were added and the cells were pulse-labeled with 6.25 μCi/ml [1,8,-3H]spermidine for 5 hours. Control cells were grown for 24 hours, treated with 5 mM DFMO for an additional 48 hours and pulse-labeled with 6.25 μMCi/ml [1,8,-$^3$H]spermidine for 5 hours after treatment with 1 mM aminoguanidine. Polyamine-depleted cells which were treated with 1 mM aminoguanidine plus 50 μM of $N^1$-guanyl-1,7-diamino-heptane (GC-7), an inhibitor of deoxyhypusine synthase (33) and pulse-labeled with 6.25 μMCi/ml [1,8,-$^3$H] spermidine for 5 hours, were used as a positive control for the inhibition of the enzymatic process of eIF5A modification. The cells were harvested with trypsin and washed twice with cold PBS. Pellets were resuspended in 800 μl of 0.1 N HCL, sonicated for 10 s at room temperature and after addition of 80 μl of 2 N perchloric acid ($HClO_4$) were incubated at 4˚C overnight. $HClO_4$-insoluble fractions were washed three times with cold 0.2 N $HClO_4$ and hydrolysed in 6 M HCl at 120˚C for 18 h. After drying under air in a hood for 6-7 h, pellets were dissolved in 500 μl of 0.2 N $HClO_4$ and separated by HPLC as described (34). Hypusine was identified as radiolabel eluting at a position of free hypusine (34). Radioactivities were measured by scintillation counting of 1-min fractions, collected from the post-column effluent supplemented with 10 ml of Ecolite (ICN, Irvine, CA, USA).

*Metabolic labeling of HCT116 cells*. Cells were grown in 100 mm dishes with or without 10 μM PG-11047 for 48 h. Media were then replaced with methionine-free media for 1 h and 3 ml of [$^{35}$S]-methionine (100 μCi/ml) were added per dish. Cells were incubated for 6 h. After completion of the labeling, the media were removed, then the cells were washed twice with PBS, lysed and counted using a scintillation counter.

*Statistics*. *P*-values between control and treated cells were calculated with ANOVA or *t*-test (Microsoft Excel, Microsoft Corp., Redmond, WA, USA).

## Results

*Effect of the polyamine analog PG-11047 on HCT116 cell growth and viability*. The sensitivity of HCT116 cells to PG-11047 was assessed by analysis of cell growth and viability. PG-11047 treatment resulted in significant growth inhibition of HCT116 cells in a time- and dose-dependent manner (Figure 2A). An almost 50% decrease in cell number was observed after a 72 h exposure to 10 μM PG-11047. In order to evaluate the long-term effect of the compound on cultured cells, we tested the viability of HCT116 cells treated with PG-11047 after seven days in culture using a Beckman Coulter Vi-Cell™ Cell Viability analyzer (Figure 2B). The total and viable cell numbers were similar at all concentrations used, except for the concentration of 1 μM where the number of viable cells decreased two-fold, suggesting a cytotoxic effect at this concentration.

*Effect of PG-11047 on gene expression*. To identify genes whose expression is regulated by PG-11047 in HCT116 cells, we used the Affymetrix Human Genome GeneChip array U133 Plus 2.0. This platform contains over 47,000 transcripts with 38,500 well-characterized human genes. We profiled the gene expression in HCT116 cells for one time point (72 h) at two different concentrations (1 and 10 μM) using results from three (for a concentration of 10 μM) or

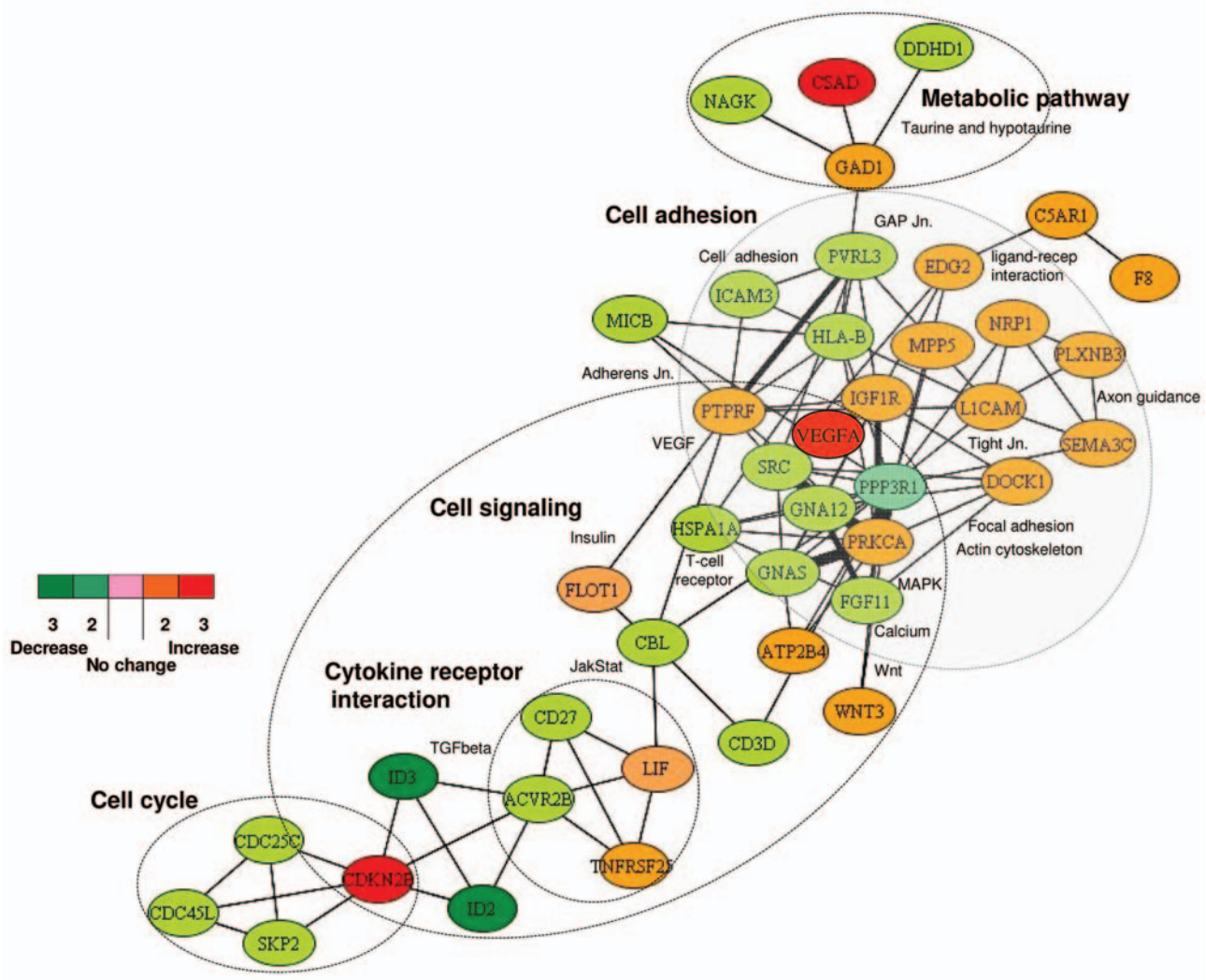


Figure 6. *Cellular pathways influenced by CGC-11047 based on Pathway Miner analysis of the KEGG pathway database. Nodes are labeled using the gene names. The color of the nodes is based on the expression values of up- and down-regulated genes. The edges indicate relationships between genes in the pathway. The edge weights indicate the number of pathways in which the associating nodes (genes) interact.*

four (for a concentration of 1 μM) independent experiments. A comparison of the distribution of gene expression patterns revealed a greater difference in cells treated with 10 μM of the analog. Three hundred and sixteen genes were altered in a statistically significant manner in HCT116 cells treated with 10 μM PG-11047, and forty-one genes were differentially expressed after treatment with a 1 μM dose of the compound. The list of genes differentially expressed in response to the dose of 10 μM was further filtered for a 3-fold change from that of the control cells. Eighty-one genes were found to be differentially expressed in PG-11047-treated cells using a 3-fold cut-off (presented in Table IA). A HeatMap of these 81 genes showing the expression profile across the ten experiments is presented in Figure 3. Selected down-or up-regulated genes whose expression was significantly changed in the Affymetrix arrays after treatment with 10 μM of PG-11047 are presented in Table IB. We confirmed these differentially expressed genes by real-time RT PCR analysis (Figure 4). The first gene presented in Table IB is early growth response gene-1 (*EGR-1*), which is a member of a family of zinc-finger transcription factors and which participates in cellular proliferation, differentiation and apoptosis (35, 36). *EGR-1* binds to a consensus GC-rich element (GCE) 5'-GCGGGGGCG-3' to regulate the transcription of numerous target genes including *TGFβ* (37), basic fibroblast growth

Table IIA. *Major PG-11047-dependent changes in cellular and regulatory pathways based on KEGG pathways resources.*

| Gene name | Biological function | Accession | Log ratio* 1 μM | Log ratio* 10 μM |
|---|---|---|---|---|
| MAPK signaling pathway | | | | |
| PPP3R1 | Protein phosphatase regulatory subunit B, alpha isoform | NM_000945 | | |
| GNA12 | Guanine nucleotide binding protein gamma 12, activity | BE504098 | | |
| PRKCA | Protein kinase C-alpha, regulation of progression through cell cycle, induction of apoptosis by extracellular signals | AI471375 | | |
| HSPA1A | Heat-shock 70 kDa protein 1A, chaperon | NM_005345 | | |
| FGF11 | Fibroblast growth factor 11, cell–cell signaling | AW172597 | | |
| Cell cycle | | | | |
| CDC45L | Cell division cycle 45-like, regulation of progression through cell cycle | NM_003504 | | |
| CDKN2B | Cyclin-dependent kinase inhibitor 2B, cell cycle arrest | AW444761 | | |
| SKP2 | S-phase kinase associated protein 2, G1/S transition of mitotic cycle | NM_005983 | | |
| CDC25C | Cell division cycle 25 homolog, regulation of mitosis, traversing start control point of mitotic cell cycle | NM_001790 | | |
| Wnt signaling pathway | | | | |
| PPP3R1 | Protein phosphatase C regulatory subunit B, calcium-dependent protein serine/threonine phosphotase activity | AL544951 | | |
| WNT3 | Wingless-type MTV integration site family, member 3, WNt receptor signaling pathway | AA463626 | | |
| PRKCA | Protein kinase C, alpha, regulation of progression through cell cycle, induction of apoptosis by extracellular signals | AI471375 | | |
| Focal adhesion, adherent and gap junction | | | | |
| SRC | v-SRC sarcoma oncogene homolog, protein amino acid phosphorylation, protein kinase cascade | BG767702 | | |
| IGF1R | Insulin-like growth factor 1 receptor, positive regulator of cell proliferation | AI830698 | | |
| DOCK1 | Dedicator of cytokinesis 1, integrin-mediated signaling pathway | AA599017 | | |
| PTPRF | Protein tyrosine phosphatase receptor type F, protein amino acid dephosphorylation | NM_002840 | | |
| PVRL3 | Poliovirus receptor related 3, cell adhesion | AA129716 | | |
| EDG2 | Endothelial differentiation, lysophosphatidic acid G-coupled receptor 2, positive regulator of NF-κB cascade | AW269335 | | |
| GNAS | GNAS complex locus, Golgi to secretory vesicle transport, protein secretion | AA401492 | | |
| DNA polymerase | | | | |
| POLE2 | Polymerase (DNA-directed) epsilon 2, DNA replication | NM_002692 | | |
| POLI | polymerase (DNA-directed) iota, DNA replication | NM_007195 | | |
| POLD1 | Polymerase DNA-directed delta 1, catalytic subunit, S-phase of mitotic cell cycle | NM_002691 | | |
| TGF beta signaling | | | | |
| ID2 | Inhibitor of DNA-binding 2, dominant negative helix-loop-helix protein | NM_002166 | | |
| CDKN2B | Cyclin-dependent kinase inhibitor 2B, cell cycle arrest | AW444761 | | |
| ID3 | Inhibitor of DNA-binding 3, negative regulator of transcription from RNA polymerase II | NM_002167 | | |
| ACVR2B | Activin A receptor type 2B, protein amino acid phosphorylation | NM_001106 | | |

Genes with altered expression and their known function(s) are indicated. *Colors indicate the range of the change in gene expression calculated as the log of the ratio of average expression in the three arrays from PG-11047-treated HCT116 cells to average expression in three arrays from control cells according to the following scheme:

Table IIB. *Genes differentially expressed in HCT116 cells treated with 1 μM PG-11047 ($p<0.05$).*

| Gene ID | Symbol | Description | Fold change Mean±SD | Function |
|---|---|---|---|---|
| 210764_s_at | CYR61 | Cysteine-rich, angiogenic inducer, 61 | 0.25±0.03 | |
| 209101_at | CTGF | Connective tissue growth factor | 0.27±0.02 | |
| 201289_at | CYR61 | Cysteine-rich, angiogenic inducer, 61 | 1.72±0.17 | |
| 201464_x_at | JUN | Jun oncogene | 0.39±0.06 | See FOS |
| 202887_s_at | DDIT4 | DNA-damage-inducible transcript 4 | 2.31±0.47 | |
| 225740_x_at | MDM4 | Mdm4, transformed 3T3 cell double minute 4, p53-binding protein (mouse) | 1.68±0.02 | Inhibits p-53 and p73-mediated cell cycle arrest and apoptosis. Inhibits degradation of MDM2 |
| 207740_s_at | NUP62 | Nucleoporin 62 kDa | 0.61±0.06 | Involved in nucleocytoplasmic transport. The C-terminal is involved in protein protein interaction. |
| 209189_at | FOS | v-fos FBJ murine osteosarcoma viral oncogene homolog | 0.08±0.02 | As the heterodimer with the JUN transcription factor, plays an important role in signal transduction, cell proliferation, and differentiation. |
| 238593_at | FLJ22531 | Hypothetical protein FLJ22531 | 3.00±0.8 | |
| 201110_s_at | THBS1 | Thrombospondin 1 | 0.45±0.07 | |
| 203168_at | CREBL1 | cAMP responsive element binding protein-like 1 | 0.7±0.01 | Act in the unfolded protein response (UPR) pathway by activating UPR target genes induced during ER stress. |

factor (*bFGF*) (38), *p53* (39), and *thymidine kinase* (40). *EGR-1* mRNA expression was found to be significantly higher in gastric cancer tissue than in normal mucosa (41). *EGR-1* has been implicated in the progression of prostate cancer since its basal expression was very low in normal prostate and elevated in prostate cancer. The *EGR-1* levels of expression also correlated directly with Gleason scores (42, 43). PG-11047 treatment resulted in a statistically significant and concentration-dependent decrease in *EGR-1* mRNA level (5- and 10- fold decrease, for 1 μM and 10 μM, respectively) (Figure 4). The other regulatory gene differentially expressed in PG-11047-treated cells was cyclin L2 (*CCNL2*), which is a novel member of the cyclin family of genes, playing a key role in transcriptional regulation (44). It was shown recently that overexpression of human cyclin L2 suppresses the growth of human lung carcinoma cell line A549 *via* induction of cell cycle arrest and apoptosis involving up-regulation of caspase 3 and down-regulation of Bcl-2 and survivin (45). The mechanism of CCNL2 activity includes regulation of the pre-mRNA splicing process, since it was found to be co-localized with splicing factors SC-35 and 9G8 (46). PG-11047 induced increased CCNL2 transcript level up to 3-fold at a dose of 10 μM, which could account in part for the growth inhibitory activity of this agent (Figure 4). The gene *SLC6A6/TauT*, which belongs to the family of Na+- and Cl-dependent neurotransmitter transporters SLC6 (47), was also induced up to 3-fold when cells were treated with 10 μM of PG-11047 (Table IB). SLC6A6/TauT is expressed in retinal capillary endothelial cells and mediates transport of taurine (48). SLC6A6/TauT also has been recognized as a

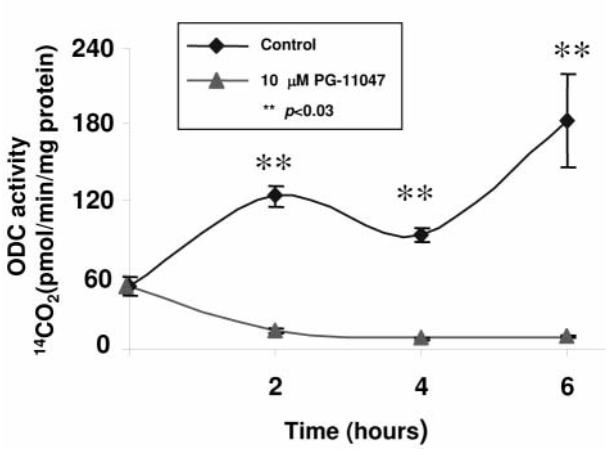


Figure 7. *ODC enzyme activity in HCT116 cells treated with 10 μM of PG-11047. HCT116 cells were grown for 24 h before adding the polyamine analog. Control cells and cells treated with PG-11047 were collected 0, 2, 4, and 6 hours after the addition of PG-11047, and ODC enzyme activity was measured as described in Materials and Methods. Measurements were carried out in triplicate. P-values between control and treated cells were calculated with t-test.*

transporter of γ-aminobutyric acid (GABA) at the inner blood-retinal barrier, at least in conditionally immortalized rat retinal capillary endothelial cells (49). SLC6A6/TauT might play an important role in the reducing the GABA concentration in the retinal interstitial fluid. We suggest that PG-11047-mediated up-regulation of this transporter could lead to an increase in GABA transport and possibly relieve the hypo-osmotic and ischaemic conditions in the retina during diseases such as diabetes. The up-regulation of

Table III. *Polyamine levels (nmol/mg protein) in HCT116 cells treated with 10 μM PG-11047. Cells were seeded with media containing the polyamine analog. Control and PG-11047-treated cells were collected at 0, 24 and 48 h after the drug addition. Results are presented as average values of three independent experiments.*

| Hours in culture | Putrescine | | $N^1$ Acetylspermidine | | Spermidine | | Spermine | |
|---|---|---|---|---|---|---|---|---|
| | Control | PG-11047 | Control | PG-11047 | Control | PG-11047 | Control | PG-11047 |
| 0 | 3.65±0.33 | 3.65±0.33 | 0.19±0.03 | 0.19±0.03 | 8.07±0.43 | 8.07±0.43 | 8.95±0.45 | 8.95±0.45 |
| 24 | 3.03±0.17 | 0.22±0.01* | 0.38±0.04 | 1.30±0.03* | 6.95±0.47 | 1.06±0.03* | 7.70±0.56 | 2.50±0.06* |
| 48 | 2.20±0.31 | 0.04±0.03* | 0.41±0.04 | 0.52±0.03 | 6.46±0.77 | 0.11±0.00* | 7.31±0.73 | 0.40±0.03* |

*$P$-value <0.01 for the difference in values between control and PG-11047-treated cells.

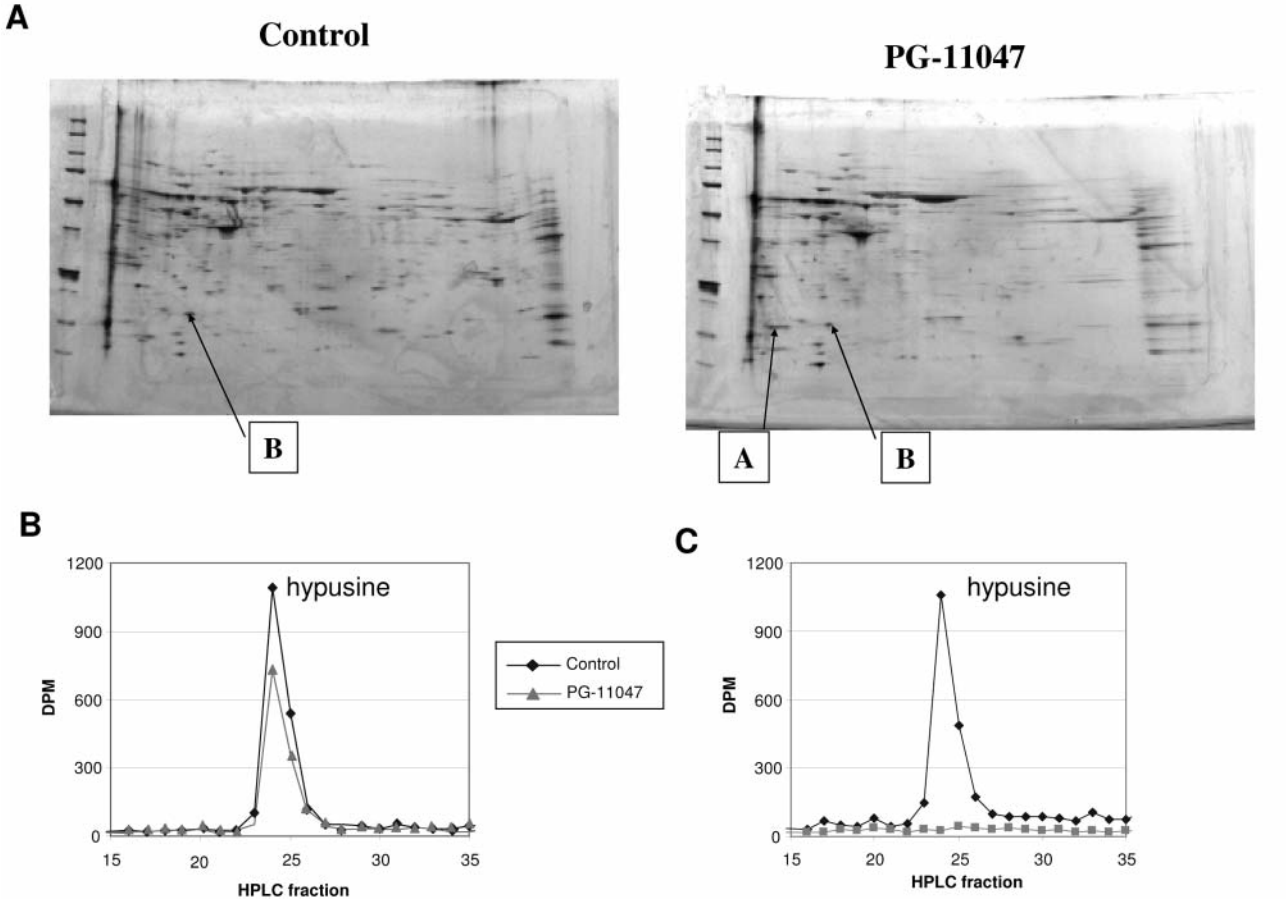


Figure 8. *PG-11047 influences the posttranslational modification of eIF5A in HCT116 colon cancer cells. A, Spots of unmodified (A) and modified (B) eIF5A in PG-11047-treated HCT116 cells separated by 2D-PAGE and stained with silver stain. Control and PG-11047-treated HCT116 cells were collected 72 h after subculture and samples were analysed using 2D PAGE gel electrophoresis as described in Materials and Methods. Images presented are from one of three independent experiments. B, Effect of PG-11047 treatment on synthesis of hypusine in HCT116 cells. HCT116 cells were grown in culture for 24 h and were then treated with 5 mM DFMO for 48 h; after that 1 mM aminoguanidine only (Control) or 1 mM aminoguanidine plus 10 μM PG-11047 (PG-treated) were added and cells were incubated in the presence of [1,8-3H]spermidine for 5 h before harvesting and processing for hypusin analysis as described in Materials and Methods. Shown is the elution or radiolabel after separation of the hydrolyzed protein sample by HPLC. The early fractions (elution times less than 15 min.) contained no radiolabel. Results presented are representative of an experiment which was repeated twice. B, Suppression of the eIF5A modification by GC-7. HCT116 cells were grown in culture for 24 h and were then treated with 5 mM DFMO; after that 1 mM aminoguanidine plus vehicle control (acetic acid) (Control) or 1 mM aminoguanidine plus 50 μM of GC-7 (GC-7) were added and cells were incubated in the presence of [1,8-$^3$H]spermidine for 5 h before harvesting and processing for hypusin analysis as described in Materials and Methods.*

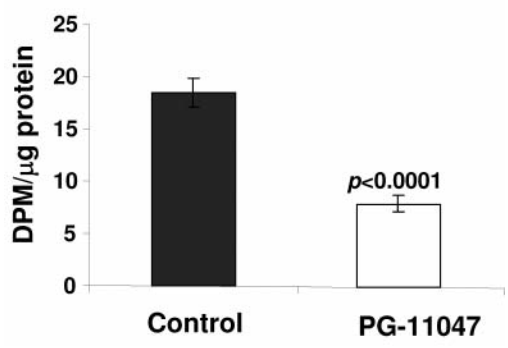


Figure 9. *General protein synthesis rate in control and PG-11047-treated HCT116 cells. Cells were treated with PG-11047 for 48 h and labeled with [$^{35}$S]-methionine as described in Materials and Methods. Results are presented as average values of three independent experiments. P-values between control and treated cells were calculated with t-test.*

*VEGF-A* gene transcript was also confirmed in PG-11047-treated HCT116 cells by real-time PCR (Figure 5A). At the same time, we found that VEGF-A protein expression was significantly lower in cells treated with 10 μM of the compound, compared to the level of expression in control cells (Figure 5B, $p$=0.006), suggesting that PG-11047 may interfere with the mechanism of VEGF translation.

We also analysed the changes in cellular pathways associated with PG-11047 treatment using Pathway Miner software (www.biorag.org) developed by the Bioinformatics Shared Service at the Arizona Cancer Center, University of Arizona (29). Using this software, we were able to identify cellular pathways affected by this polyamine analog (Figure 6 and Table IIA). The altered genes were involved in MAPK signaling, Wnt signaling, TGF beta signaling, cytokine receptor interaction, the cell cycle and cell adhesion.

Assessing the effect of PG-11047 on cell viability, we found an unusual decrease in the number of viable cells when HCT116 cells were treated with a 1 μM dose of the compound. In order to determine whether any differences in gene expressions account for the observed dose effect in cell viability, we compared the gene expression in control cells and in 1 μM- and 10 μM-treated cells. Eleven genes were identified as uniquely altered in cells treated with the 1 μM dose. These genes are presented in Table IIB. It remains to be determined which of these genes or their combinations may contribute to the observed physiological effect.

*Effect of PG-11047 on genes involved in polyamine metabolism in HCT116 colon cancer cells.* The inhibitory effect of PG-11047 on polyamine metabolism, which occurs *via* suppression of activity of the polyamine biosynthetic enzyme ODC and induction of a key polyamine catabolic enzyme SAT1, has been reported in several lung cancer cell lines (24). Similarly, we found that SAT1 was significantly up-regulated in HCT116 colon cancer cells after treatment with PG-11047 (6.46±1.9 fold change, Table IB). Validation using real-time RT PCR confirmed a concentration-dependent induction of *SAT1* gene expression by this analog ($p$=0.017) (Figure 4). ODC enzyme activity was suppressed starting as early as 2 hours after addition of the analog ($p$<0.03) (Figure 7), presumably due to the stimulation of antizyme production by PG-11047 (27). Subsequently, putrescine, spermidine and spermine levels were significantly lower in PG-11047-treated HCT116 cells ($p$<0.01) (Table III), leading to a 14-fold decrease in the total polyamine content after the 48 h of treatment (17.21±1.98 nmol/mg protein in control cells *vs*. 1.21±0.04 nmol/mg protein in PG-11047-treated cells).

*Cellular effects of PG-11047.* While performing the analysis of changes in protein expression after treatment with PG-11047 using proteomic techniques, we identified the presence of the unmodified eukaryotic translation initiation factor 5A (eIF5A, gi number 109296) on 2D PAGE gels run from samples treated with PG-11047 (Figure 8A). eIF5A is a putatitive eukaryotic translation initiation factor that is modified postranslationally by the polyamine spermidine. The eIF5A modification is catalyzed by deoxyhypusine synthase, which transfers the 4-aminobutyl moiety from spermidine to the ε-amino acid deoxyhypusine. Deoxyhypusine is further hydrolysed by deoxyhypusine hydrolase to form the mature hypusine-containing eIF5A (50). Hypusine-containing eIF5A is essential for eukaryotic cell proliferation (51). To confirm the proteomics findings, we analysed hypusine production in control and PG-11047-treated HCT116 cells using an HPLC method as described in the Materials and Methods section. When PG-11047 and [1,8,-$^{3}$H]spermidine were added to the polyamine-depleted HCT116 cells hypusine production was not significantly affected, implying that PG-11047 does not inhibit the enzymatic process of eIF5A modification (Figure 8B). As a positive control for the enzymatic inhibition of hypusine synthesis we used polyamine-depleted HCT116 cells which were treated with the inhibitor of deoxyhypusine synthase CG-7 plus radiolabeled spermidine. In contrast to PG-11047-treated cells, hypusine formation was completely abolished in CG-7-treated cells (Figure 8C). Based on the results of this experiment, we explained the presence of the unmodified eIF5A in PG-11047-treated HCT116 cells found during the proteomics analysis by the depletion of spermidine, a substrate for eIF5A modification, caused by PG-11047 treatment. As a consequence, the general rate of translation in PG-11047-treated cells was suppressed ($p$<0.0001) (Figure 9).

Another protein found to be present in PG-11047-treated HCT116 cells was peroxiredoxin 5 (gi number 6746557). Peroxiredoxin 5 is a peroxisomal membrane protein which plays an important role in modulating the cellular response to hydrogen peroxide-induced stress by reducing hydrogen peroxide and alkyl hydroperoxidases (52). Overexpression of peroxiredoxin 5 may reduce mitochondrial DNA damage, thus protecting cells against apoptosis (53). Indeed, we did not detect any apoptosis in PG-11047-treated HCT116 cells by annexin V followed by flow cytometry (data not shown).

## Discussion

In recent years, interest has increased in using synthetic polyamine analogs for antineoplastic therapy (19). Several classes of polyamine analogs have been developed, including symmetrically substituted *bis*(alkyl) analogs, asymmetrically substituted analogs, and conformationally restricted analogs. These have been evaluated in cell culture and clinical trials. The conformationally restricted analog PG-11047 was well tolerated in phase I and II clinical trials in patients with lymphoma and solid tumors, therefore understanding the mechanism of antitumor action of this drug in different types of cancer has become important. As such, we conducted genome-wide gene expression profiling and proteomics assessment of HCT116 colon adenocarcinoma cells treated with this agent.

Using Pathway Miner (www.biorag.org) (29), the web-based analytical software which allows for analysis of gene expression patterns based on metabolic, cellular, and regulatory pathways, we determined that genes differentially expressed in PG-11047-treated HCT116 cells are involved in the cell cycle, focal adhesion, adherent and gap junction formation, as well as, MAPK-, Wnt-, TGF-beta signaling pathways. Eighty-one genes were altered 3-fold or more when cells were treated with 10 μM PG-11047. We validated the agent-induced three-fold alterations in expression of *EGR-1, cyclin L2a, SLC6A6/TauT,* and *SAT1*. The inhibitory effect of PG-11047 on *EGR-1* is especially important since *EGR-1* is a pivotal gene that initiates early signal transduction events in response to many stresses, including ionizing radiation and EGFR activation (54). Similarly to other cell types, PG-11047 depleted polyamine levels in HCT116 cells *via* the induction of *SAT1* gene expression and suppression of ODC enzyme activity. Treatment with a low, 1 μM dose of PG-11047 resulted in a decrease in cell viability, which was likely mediated by changes in the expression of specific genes.

Proteomics analysis revealed accumulation of unmodified eIF5A protein in PG-11047-treated cells. Quantification of hypusine synthesized in control and PG-11047-treated cells showed no significant changes in its level in treated cells provided spermidine was available for the reaction of eIF5A modification. We confirmed that PG-11047 depletes cellular spermidine, decreasing the substrate for the modification reaction and causing cells to accumulate unmodified eIF5A. This accumulation is similar to that reported in different cell types when spermidine was depleted with either DFMO (32, 55, 56) or 5'-{[(Z)-4-amino-2-butenyl]methyamino}-5'-deoxyadenosine, which blocks spermidine synthesis by inhibiting S-adenosylmethionine decarboxylase (57). The decrease of the modified eIF-5A levels resulted in the suppression of general protein synthesis in PG-11047-treated cells.

Previously, we conducted a similar gene expression analysis in HCT116 cells treated with the conformationally restricted polyamine analog PG-11093 (formerly CGC-11093) (21). Although these two agents belong to the same class of synthetic polyamine analogs, clearly small structural differences significantly modify their molecular activities. PG-11047 is an unsaturated *cis* double-bond variant of the symmetrically substituted polyamine analog $N^1$,$N^{12}$*bis*(ethyl)spermine (BESpm), and PG-11093 is a cyclopropyl variant of another symmetrically substituted polyamine analog, $N^1N^{14}$*bis*(ethyl)homospermine (BENspm). Both agents significantly deplete intracellular polyamine levels, but only PG-11047 is an effective inducer of *SAT1* transcription. Comparison of the gene expression profiles of HCT116 cells treated with CGC-11093 and PG-11047 showed that these agents act within similar signaling pathways but alter the expression of distinct genes.

In conclusion, PG-11047 exerts a strong cytostatic effect on HCT116 colon cancer cells by influencing the expression of growth-related genes and suppressing general protein synthesis. The dramatic effect of this agent on polyamine catabolism suggests that this agent could be successfully used in combination with established drugs, such as DFMO, for the targeted depletion of polyamine levels and suppression of tumor growth.

## Acknowledgements

This research was supported by Progen Pharmaceuticals, Inc. and a grant from the USPHS, NIH/NCI CA123065. The authors gratefully acknowledge the Genomics and Proteomics Shared Services at the University of Arizona for their assistance in data collection and analysis. We also acknowledge the online resource BioRag (Bioresource for array genes) at www.biorag.org, which is supported by the Arizona Cancer Center Bioinformatics Core. This work was supported by Progen Pharmaceuticals Inc., Redwood City, CA and USPHS grants CA23074 and CA95060.

## References

1 Heby O: Role of polyamines in the control of cell proliferation and differentiation. Differentiation *19*: 1-20, 1981.

2 Janne J, Alhonen L and Leinonen P: Polyamines: from molecular biology to clinical applications. Ann Med *23*: 241-259, 1991.

3 Tabor CW and Tabor H: Polyamines. Annu Rev Biochem *53*: 749-790, 1984.

4 Igarashi K and Kashiwagi K: Polyamines: mysterious modulators of cellular functions. Biochem Biophys Res Commun *271*: 559-564, 2000.

5 Matsufuji S, Matsufuji T, Miyazaki Y, Murakami Y, Atkins JF, Gesteland RF and Hayashi S: Autoregulatory frameshifting in decoding mammalian ornithine decarboxylase antizyme. Cell *80*: 51-60, 1995.

6 Lux GD, Marton LJ and Baylin SB: Ornithine decarboxylase is important in intestinal mucosal maturation and recovery from injury in rats. Science *210*: 195-198, 1980.

7 McCormack SA and Johnson LR: Polyamines and cell migration. J Physiol Pharmacol *52*: 327-349, 2001.

8 Wallace HM and Caslake R: Polyamines and colon cancer. Eur J Gastroenterol Hepatol *13*: 1033-1039, 2001.

9 Giardiello FM, Hamilton SR, Hylind LM, Yang VW, Tamez P and Casero RA Jr: Ornithine decarboxylase and polyamines in familial adenomatous polyposis. Cancer Res *57*: 199-201, 1997.

10 Erdman SH, Ignatenko NA, Powell MB, Blohm-Mangone KA, Holubec H, Guillen-Rodriguez JM and Gerner EW: APC-dependent changes in expression of genes influencing polyamine metabolism, and consequences for gastrointestinal carcinogenesis, in the Min mouse. Carcinogenesis *20*: 1709-1713, 1999.

11 Fultz KE and Gerner EW: APC-dependent regulation of ornithine decarboxylase in human colon tumor cells. Mol Carcinog *34*: 10-18, 2002.

12 Nigro ND, Bull AW and Boyd ME: Inhibition of intestinal carcinogenesis in rats: effect of difluoromethylornithine with piroxicam or fish oil. J Natl Cancer Inst 77: 1309-1313, 1986.

13 Pereira MA and Khoury MD: Prevention by chemopreventive agents of azoxymethane-induced foci of aberrant crypts in rat colon. Cancer Lett *61*: 27-33, 1991.

14 Alberts DS, Dorr RT, Einspahr JG, Aickin M, Saboda K, Xu MJ, Peng YM, Goldman R, Foote JA, Warneke JA, Salasche S, Roe DJ and Bowden GT: Chemoprevention of human actinic keratoses by topical 2-(difluoromethyl)-dl-ornithine. Cancer Epidemiol Biomarkers Prev *9*: 1281-1286, 2000.

15 Basuroy UK and Gerner EW: Emerging concepts in targeting the polyamine metabolic pathway in epithelial cancer chemoprevention and chemotherapy. J Biochem *139*: 27-33, 2006.

16 Meyskens FLJ, McLaren CE, Pelot D, Fujikawa-Brooks S, Carpenter PM, Hawk E, Kelloff G, Lawson MJ, Kidao J, McCracken J, Albers CG, Ahnen DJ, Turgeon DK, Goldschmid S, Lance P, Hagedorn CH and Gerner EW: Difluoromethylornithine plus sulindac for the prevention of sporadic colorectal adenomas: A randomized placebo controlled, double-blind trial. Cancer Prev Res *1*: 32-38, 2008.

17 Simoneau AR, Gerner EW, Nagle R, Ziogas A, Fujikawa-Brooks S, Yerushalmi H, Ahlering TE, Lieberman R, McLaren CE, Anton-Culver H and Meyskens FLJ: The effect of difluoromethylornithine on decreasing prostate size and polyamines in men: results of a year-long phase IIb randomized placebo-controlled chemoprevention trial. Cancer Epidemiol Biomarkers Prev *17*: 292-299, 2008.

18 Seiler N: Pharmacological aspects of cytotoxic polyamine analogs and derivatives for cancer therapy. Pharmacol Ther *107*: 99-119, 2005.

19 Casero RA Jr and Marton LJ: Targeting polyamine metabolism and function in cancer and other hyperproliferative diseases. Nat Rev Drug Discov *6*: 373-390, 2007.

20 Huang Y, Pledgie A, Casero RA Jr and Davidson NE: Molecular mechanisms of polyamine analogs in cancer cells. Anticancer Drugs *16*: 229-241, 2005.

21 Ignatenko NA, Yerushalmi HF, Watts GS, Futscher BW, Stringer DE, Marton LJ and Gerner EW: Pharmacogenomics of the polyamine analog 3,8,13,18-tetraaza-10,11-[(E)-1,2-cyclopropyl]eicosane tetrahydrochloride, CGC-11093, in the colon adenocarcinoma cell line HCT1161. Technol Cancer Res Treat *5*: 553-564, 2006.

22 Reddy VK, Valasinas A, Sarkar A, Basu HS, Marton LJ and Frydman B: Conformationally restricted analogues of $^{1}N$,$^{12}N$-bisethylspermine: synthesis and growth inhibitory effects on human tumor cell lines. J Med Chem *41*: 4723-4732, 1998.

23 Valasinas A, Sarkar A, Reddy VK, Marton LJ, Basu HS and Frydman B: Conformationally restricted analogues of $^{1}N$,$^{14}N$-bisethylhomospermine (BE-4-4-4): synthesis and growth inhibitory effects on human prostate cancer cells. J Med Chem *44*: 390-403, 2001.

24 Hacker A, Marton LJ, Sobolewski M and Casero RA Jr: *In vitro* and *in vivo* effects of the conformationally restricted polyamine analogue CGC-11047 on small cell and non-small cell lung cancer cells. Cancer Chemother Pharmacol *63*: 45-53, 2008.

25 Holst CM, Frydman B, Marton LJ and Oredsson SM: Differential polyamine analogue effects in four human breast cancer cell lines. Toxicology *223*: 71-81, 2006.

26 Reddy BS: Prevention of colon cancer by pre- and probiotics: evidence from laboratory studies. Br J Nutr *80*: S219-223, 1998.

27 Mitchell JL, Thane TK, Sequeira JM, Marton LJ and Thokala R: Antizyme and antizyme inhibitor activities influence cellular responses to polyamine analogs. Amino Acids *33*: 291-297, 2007.

28 Lima e Silva R, Kachi S, Akiyama H, Shen J, Hatara MC, Aslam S, Gong YY, Khu NH, Lauer TW, Hackett SF, Marton LJ and Campochiaro PA: Trans-scleral delivery of polyamine analogs for ocular neovascularization. Exp Eye Res *83*: 1260-1267, 2006.

29 Pandey R, Guru RK and Mount DW: Pathway Miner: extracting gene association networks from molecular pathways for predicting the biological significance of gene expression microarray data. Bioinformatics *20*: 2156-2158, 2004.

30 Sertich GJ, Glass JR, Fuller DJ and Gerner EW: Altered polyamine metabolism in Chinese hamster cells growing in a defined medium. J Cell Physiol *127*: 114-120, 1986.

31 Seiler N and Knodgen B: High-performance liquid chromatography procedure for the simultaneous determination of the natural polyamines and their monoacetylderivatives. J. Chromatography *221*: 227-238, 1980.

32 Gerner EW, Mamont PS, Bernhardt A and Siat M: Post-translational modification of the protein-synthesis initiation factor eIF-4D by spermidine in rat hepatoma cells. Biochem J *239*: 379-386, 1986.

33 Lee CH and Park MH: Human deoxyhypusine synthase: interrelationship between binding of NAD and substrates. Biochem J *352(Pt 3)*: 851-857, 2000.

34 Murphey RJ and Gerner EW: Hypusine formation in protein by a two-step process in cell lysates. J Biol Chem *262*: 15033-15036, 1987.

35 Milbrandt J: A nerve growth factor-induced gene encodes a possible transcriptional regulatory factor. Science *238*: 797-799, 1987.

36 Sukhatme VP, Cao XM, Chang LC, Tsai-Morris CH, Stamenkovich D, Ferreira PC, Cohen DR, Edwards SA, Shows TB, Curran T *et al*: A zinc finger-encoding gene coregulated with c-fos during growth and differentiation, and after cellular depolarization. Cell *53*: 37-43, 1988.
37 Kim SJ, Park K, Rudkin BB, Dey BR, Sporn MB and Roberts AB: Nerve growth factor induces transcription of transforming growth factor-beta 1 through a specific promoter element in PC12 cells. J Biol Chem *269*: 3739-3744, 1994.
38 Biesiada E, Razandi M and Levin ER: *Egr-1* activates basic fibroblast growth factor transcription. Mechanistic implications for astrocyte proliferation. J Biol Chem *271*: 18576-18581, 1996.
39 Bingham SA, Day NE, Luben R, Ferrari P, Slimani N, Norat T, Clavel-Chapelon F, Kesse E, Nieters A, Boeing H, Tjonneland A, Overvad K, Martinez C, Dorronsoro M, Gonzalez CA, Key TJ, Trichopoulou A, Naska A, Vineis P, Tumino R, Krogh V, Bueno-de-Mesquita HB, Peeters PH, Berglund G, Hallmans G, Lund E, Skeie G, Kaaks R and Riboli E: Dietary fibre in food and protection against colorectal cancer in the European Prospective Investigation into Cancer and Nutrition (EPIC): an observational study. Lancet *361*: 1496-1501, 2003.
40 Molnar G, Crozat A and Pardee AB: The immediate-early gene *Egr-1* regulates the activity of the *thymidine kinase* promoter at the G0-to-G1 transition of the cell cycle. Mol Cell Biol *14*: 5242-5248, 1994.
41 Kobayashi D, Yamada M, Kamagata C, Kaneko R, Tsuji N, Nakamura M, Yagihashi A and Watanabe N: Overexpression of early growth response-1 as a metastasis-regulatory factor in gastric cancer. Anticancer Res *22*: 3963-3970, 2002.
42 Eid MA, Kumar MV, Iczkowski KA, Bostwick DG and Tindall DJ: Expression of early growth response genes in human prostate cancer. Cancer Res *58*: 2461-2468, 1998.
43 Thigpen AE, Cala KM, Guileyardo JM, Molberg KH, McConnell JD and Russell DW: Increased expression of early growth response-1 messenger ribonucleic acid in prostatic adenocarcinoma. J Urol *155*: 975-981, 1996.
44 Bregman DB, Pestell RG and Kidd VJ: Cell cycle regulation and RNA polymerase II. Front Biosci *5*: D244-257, 2000.
45 Li HL, Wang TS, Li XY, Li N, Huang DZ, Chen Q and Ba Y: Overexpression of cyclin L2 induces apoptosis and cell-cycle arrest in human lung cancer cells. Chin Med J (Engl) *120*: 905-909, 2007.
46 Yang L, Li N, Wang C, Yu Y, Yuan L, Zhang M and Cao X: Cyclin L2, a novel RNA polymerase II-associated cyclin, is involved in pre-mRNA splicing and induces apoptosis of human hepatocellular carcinoma cells. J Biol Chem *279*: 11639-11648, 2004.
47 Gether U, Andersen PH, Larsson OM and Schousboe A: Neurotransmitter transporters: molecular function of important drug targets. Trends Pharmacol Sci *27*: 375-383, 2006.
48 Tomi M, Terayama T, Isobe T, Egami F, Morito A, Kurachi M, Ohtsuki S, Kang YS, Terasaki T and Hosoya K: Function and regulation of taurine transport at the inner blood-retinal barrier. Microvasc Res *73*: 100-106, 2007.
49 Tomi M, Tajima A, Tachikawa M and Hosoya K: Function of taurine transporter (Slc6a6/TauT) as a GABA transporting protein and its relevance to GABA transport in rat retinal capillary endothelial cells. Biochim Biophys Acta *1778*: 2138-2142, 2008.
50 Park MH, Cooper HL and Folk JE: The biosynthesis of protein-bound hypusine (*N* epsilon-(4-amino-2-hydroxybutyl)lysine). Lysine as the amino acid precursor and the intermediate role of deoxyhypusine (*N* epsilon-(4-aminobutyl)lysine). J Biol Chem *257*: 7217-7222, 1982.
51 Park MH, Lee YB and Joe YA: Hypusine is essential for eukaryotic cell proliferation. Biol Signals *6*: 115-123, 1997.
52 Yamashita H, Avraham S, Jiang S, London R, Van Veldhoven PP, Subramani S, Rogers RA and Avraham H: Characterization of human and murine PMP20 peroxisomal proteins that exhibit antioxidant activity *in vitro*. J Biol Chem *274*: 29897-29904, 1999.
53 Banmeyer I, Marchand C, Clippe A and Knoops B: Human mitochondrial peroxiredoxin 5 protects from mitochondrial DNA damages induced by hydrogen peroxide. FEBS Lett *579*: 2327-2333, 2005.
54 Tsai JC, Liu L, Guan J and Aird WC: The *Egr-1* gene is induced by epidermal growth factor in ECV304 cells and primary endothelial cells. Am J Physiol Cell Physiol *279*: C1414-1424, 2000.
55 Park MH: Regulation of biosynthesis of hypusine in Chinese hamster ovary cells. Evidence for eIF-4D precursor polypeptides. J Biol Chem *262*: 12730-12734, 1987.
56 Tome ME and Gerner EW: Hypusine modification in eukaryotic initiation factor 5A in rodent cells selected for resistance to growth inhibition by ornithine decarboxylase-inhibiting drugs. Biochem J *320(Pt 1)*: 55-60, 1996.
57 Byers TL, Wiest L, Wechter RS and Pegg AE: Effects of chronic 5'-([(Z)-4-amino-2-butenyl]methylamino)-5'-deoxy- adenosine (AbeAdo) treatment on polyamine and eIF-5A metabolism in AbeAdo-sensitive and -resistant L1210 murine leukaemia cells. Biochem J *290(Pt 1)*: 115-121, 1993.

*Received February 10, 2009*
*Accepted March 26, 2009*